ELECTROMAGNETIC BANDGAP WAVEGUIDE FILTERS FOR MICROWAVE AND OPTICAL APPLICATIONS

Richard W. Ziolkowski
Department of Electrical & Computer Engineering
The University of Arizona, 1230 E. Speedway
Tucson, AZ 85721-0104
E-mail: ziolkowski@ece.arizona.edu

1. Introduction

Numerous research groups are using electromagnetic bandgap (EBG) strutures to modify the performance of passive and active microstrip fed patch antennas. Analogously, nanometer and micron sized optical photonic bandgap (PBG) devices are currently being explored for their applications in a variety of systems associated with communications, data storage, optical computing, etc. The PBG structure has become a very important subject in the optics regime, for example, for microcavity laser mirrors and filters [1]. It has been demonstrated that EBG/PBG structures can be used in all of these frequency regimes to form extremely narrow bandwidth filters and extremely small waveguiding structures [1-3]. The ability of the FDTD approach (see [4, 5] for extensive reviews on this approach and its applications) to model finite-sized EBG/PBG structures with the defects required to form these filters and waveguides, has been demonstrated by several research groups. Our FDTD simulator has been extended recently to study material dispersive effects in EBG/PBG structures[6]. This allowed the study of metallo-dielectric EBG/PBG structures; i.e., layered structures formed from alternating layers of dielectrics and metals. In particular, dispersive effects occur at optical frequencies even for copper, silver, or gold conductors. This is due to the fact that at such high frequencies, the imaginary part of the index of refraction can be larger than its real part. A Lorentz material model for the metal is needed rather than a simple conductivity model and was readily included in the FDTD simulator.

This paper investigates the use of EBG/PBG waveguiding structures for microwave and optical filtering operations. It has been demonstrated computationally and experimentally that EBG/PBG structures can be used to form nanometer-sized waveguiding structures. The FDTD simulator used in the present EBG/PBG waveguide analysis has been validated previously [2, 3] and dealt with basic sub-wavelength waveguiding structures in square and triangular EBG/PBGs formed in a dielectric substrate with air holes and fed by dielectric waveguides as well as free-space beams scattering from EBG/PBGs formed from a set of dielectric rods. These structures have potential applications in the microwave and millimeter-wave regime as well as for integrated optics. Waveguide channels in regular EBG/PBG structures are formed by the removal of particular sets of rods. The triangular EBG/PBG structures lend themselves to the design of Y-power splitters. Square EBG/PBG structures with circular and square rods more naturally lead to the filter applications considered here. By introducing further defects into the EBG/PBG structures, we have demonstrated that control of the electromagnetic power flow in these EBG/PBG waveguides can be achieved and that with such additional defects, defect-based switches can be realized [2,3].

The basic waveguide band-pass filter is designed and several cases are presented to illustrate that the filter location depends on the properties of the EBG/PBG structure. All of these structures are characterized with our EBG/PBG structure FDTD simulator. Square EBG/PBG structures with circular and square metal rods and circular and square air holes are considered and contrasted. Only results for lossless and lossy dielectric rods are presented; dispersive rods results are currently under investigation. It is then demonstrated that these filters can

be successfully cascaded together in the same structure to achieve multiple null transmission windows.

2. Simulator

The EBG/PBG structures considered consist of an EBG/PBG structure formed in a dielectric block by embedding dielectric and metallic posts within it. The EBG/PBG structure is fed with one dielectric waveguide; it has a single output port that consists of a dielectric waveguide of the same type. Only semi-infinite (2D) EBG/PBG structures were considered for this study. The slab waveguides and the rods/holes are oriented with their infinite dimension along the y-axis. The FDTD simulations were then restricted to the TM case (E_y, H_x, and H_z field components) since this field configuration allows the EBG/PBG structure to have its largest effect when the rods are metal, i.e., the electric field becomes extremely small on the high conductivity cylinders. They will thus force a large perturbation in the electric field distribution within the dielectric block. The incident waveguide field is launched from a total field/scattered field boundary; the initial spatial distribution is defined by the lowest order, dominant dielectric waveguide mode. The simulation region is terminated with the lossy 2TDLM ABC (absorbing boundary condition) [6,7]. This allows the input and output dielectric waveguides to be extended completely into the ABC regions.

The EBG/PBG structure consists of a square lattice with $M columns \times N rows$ of circular and square cylinders embedded in the dielectric block. The basic configuration is shown in Fig. 1. In all cases the FDTD cells were square with an edge length of $\Delta = \lambda_0/100$, where λ_0 is the free space wavelength. For the optical simulations the center frequency was set at $f_0 = 2.0 \times 10^{14}\, Hz$ so that $\lambda_0 = 1.5\, \mu m$. The distance between the centers of each post is a; the circular rods have a diameter of $2r$ while the square rods have a sidelength of $2r$. The simulations were run with Δt at the Courant limit for $10,000$ time steps.

We characterized the electromagnetic behavior of the EBG/PBG and the resulting waveguide structures by various power transmission and reflection coefficients. They were obtained by measuring the electric and magnetic fields on specified surfaces in the FDTD mesh, fast Fourier transforming these time histories, and then forming the total time-averaged Poynting's vector through those surfaces. Thus, with one broad bandwidth pulse simulation the frequency domain transfer function of the finite EBG/PBG structure was generated.

In all cases the waveguide is taken to be 20 cells wide and the background permittivity was set to that of GaAs at f_0 which means $\epsilon = 11.43\, \epsilon_0$. The width of the waveguide is thus slightly larger than half of the center wavelength in the dielectric. The loss tangent in the metal rods was set at 10^6 and the dielectric holes were air-filled. The slab waveguide solution is solved with the indicated parameters and the guidance condition for the lowest order spatial mode is obtained. The input waveguide is then excited at the total field / scattered field boundary with that spatial mode times a broad bandwidth (3 cycle) time pulse centered about f_0. The broad bandwidth output data is collected at specified locations throughout the simulation region.

3. Results

Figure 2 shows the frequency response for three filters constructed from a square lattice of metallic circular rods. These power spectra are plotted against the relative frequency referred to f_0. The EBG/PBG structure consisted of 11 *columns* $\times$ 31 *rows* , the center column being replaced by the slab waveguide. The distance between the centers and the radii of the metal posts were, respectively, $a = 14$ and $r = 4$, $a = 16$ and $r = 6$, and $a = 19$ and $r = 9$. One can see that the thicker rods pushed the center of the filter response to lower values. It was found that most of the energy not found in the output power was reflected from the filter back into the input waveguide. There was also some power scattered away from the filter. It takes some time before the waveguide mode realizes the entire EBG/PBG structure is present and, hence, responds to the presence of the filter. Consequently, some scattering will occur as the power outside of the dielectric waveguide first sees the structure. From Fig. 2 it is seen that these metallo-dielectic EBG/PBG filters are very effective, broadband response transmission passband

filters. The $a = 19$ and $r = 9$ and the $a = 16$ and $r = 6$ filters were then combined "front-to-back" in the dielectric block. The filter response of the composite structure was essentially the superposition of the two filter responses shown in Fig. 2.

Figure 3 shows the frequency responses for two EBG/PBG filters constructed from $11 columns \times 31 rows$ of circular (1) metallic rods and (2) air holes, with $a = 16$ and $r = 6$. These power spectra are plotted against the relative frequency referred to f_0. In contrast to the metal rod case it is seen that the dielectric rod (air hole) EBG/PBG filter has a much more complicated frequency response. What is interesting about this type of filter is that several reflection and transmission lines are allowed at the same time. This type of in-line filter is an excellent candidate for WDM (wavelength division multiplexing) applications.

Figure 4 shows the frequency responses for two EBG/PBG filters constructed from $11 columns \times 50 rows$ of square (1) metallic rods and (2) air holes, with $a = 14$ and $r = 4$. These power spectra are plotted against the relative frequency referred to f_0. It was found that to achieve similar transmission rejection response levels to the circular rod cases, more rows of square rods and smaller r values were required. More rows allowed more filtering to occur; more distance between the posts allowed more energy to interact with the EBG/PBG structure. Noticed that the filter lines are narrower in the square rod cases than their circular rod counterparts. This allows a more selective notched filter to occur. This also allows more filter lines to occur in the given bandwidth for the air hole case.

Similar results were obtained for the corresponding millimeter cases based on $f_0 = 100\,GHz$ and $\epsilon = 12.9$. This was to be expected since the values of a and r were selected in reference to λ_0, i.e., the filter responses were designed based on the choice of λ_0.

4. Conclusions

These results demonstrate that an integrated microwave and optics EBG/PBG based filters can be achieved in EBG/PBG waveguiding environments. Filter responses based upon EBG/PBG structures were obtained with FDTD simulations for circular and square metallic rods and for circular and square air holes. Their responses were compared and contrasted. It was also demonstrated that cascaded notched EBG/PBG based filters are possible.

Even more complicated EBG/PBG configurations can be modeled with the FDTD approach. In particular, more complex materials and structures are readily included. This flexibility of the FDTD simulator makes it a very useful design tool to study EBG/PBG based devices.

This work was supported in part by the Air Force Office of Scientific Research, Air Force Materiel Command, USAF, under grant number F49620-96-1-0039.

1. J. D. Joannopoulos, R. D. Meade, and J. N. Winn, *Phtonics Crystals: Molding the Flow of Light*, Princeton University Press, Princeton, NJ, 1995.

2. R. W. Ziolkowski and M. Tanaka, "Finite-difference time-domain modeling of dispersive material photonic band-gap structures," *J. Opt. Soc. Am. A*, vol. 16 (4), pp. 930-940, April 1999.

3. R. W. Ziolkowski and M. Tanaka, "FDTD analysis of PBG waveguide power splitters and switches for integrated optics applications," in *Integrasted Photonics Research*, OSA Technical Digest (Optical Society of America, Washington, DC, 1999), pp. 194-196.

4. A. Taflove, *Computational Electrodynamics*, Artech House, Norwood, MA, 1995.

5. A. Taflove, *Advances in Computational Electrodynamics*, Artech House, Norwood, MA, 1998.

6. R. W. Ziolkowski and M. Tanaka, "FDTD Analysis of PBG Waveguides, Power Splitters, and Switches," *Opt. Quan. Electr.*, vol. 31, pp. 843-855, October 1999.

7. D.C. Wittwer and R. W. Ziolkowski, "Two Time-Derivative Lorentz Material (2TDLM) Formulation of a Maxwellian Absorbing Layer Matched to a Lossy Medium," to appear in *IEEE Trans. Antennas and Propagat.*, February 2000.

8. D.C. Wittwer and R. W. Ziolkowski, "Maxwellian Material Based Absorbing Boundary Conditions for Lossy Media in 3D," to appear in *IEEE Trans. Antennas and Propagat.*, February 2000.

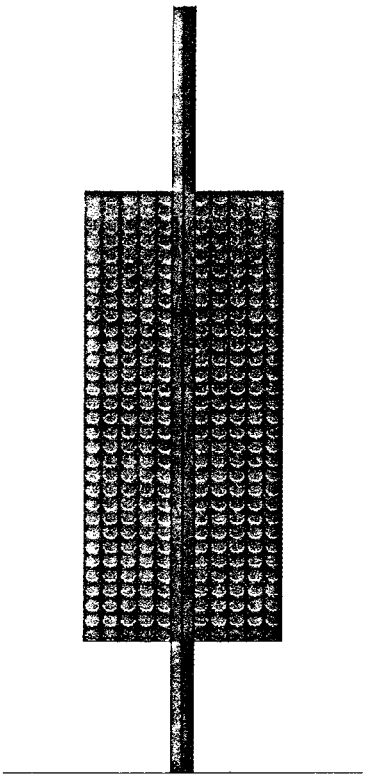

Figure 1: Square lattice EBG/PBG waveguide filter configuration

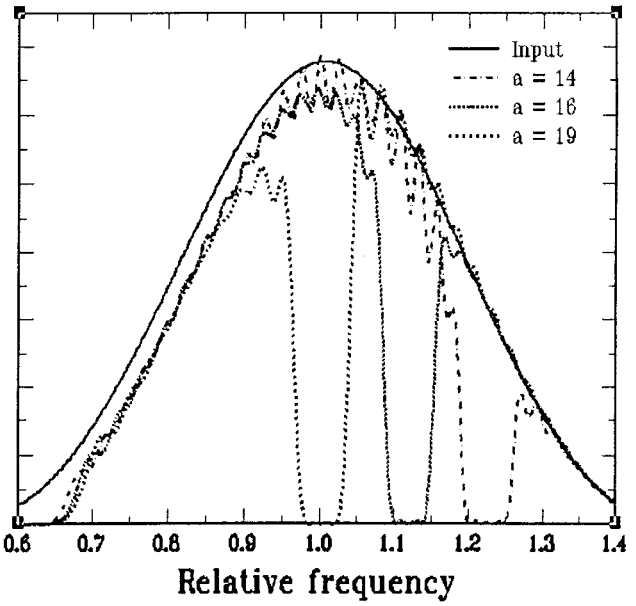

Figure 2: Power transmission spectra versus relative frequency. Filter response for three metallic circular rod square lattice EBG/PBG structures.

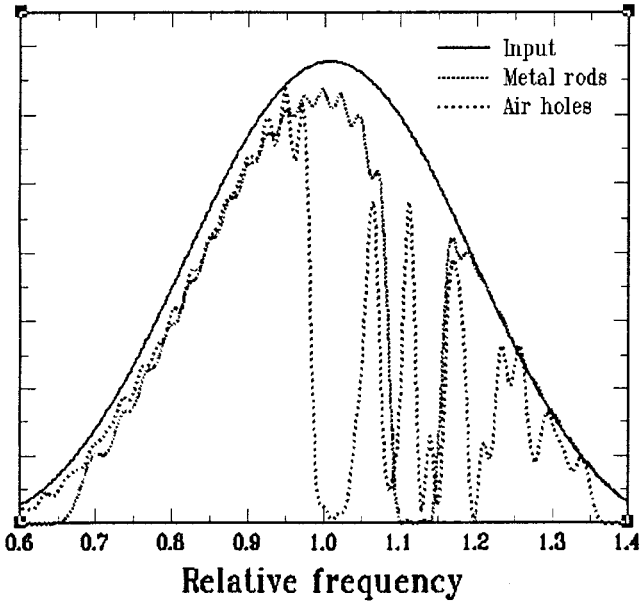

Figure 3: Power transmission spectra versus relative frequency. Filter response for corresponding circular metallic rod and air hole square lattice EPG/PBG structures.

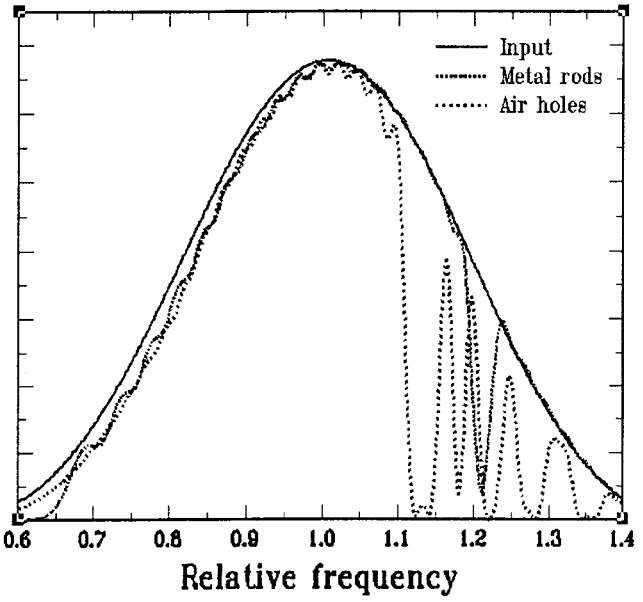

Figure 4: Power transmission spectra versus relative frequency. Filter response for corresponding square metallic rod and air hole square lattice EPG/PBG structures.